In-situ quantitative detection of irreversible lithium plating within full-lifespan of lithium-ion batteries

Heze You[a,b], Bo Jiang[a,c], Jiangong Zhu[a,b], Xueyuan Wang[a,b], Gaoya Shi[a,b], Guangshuai Han[d,e], Xuezhe Wei[a,b], Haifeng Dai[a,b,*]

[a] *School of Automotive Studies, Tongji University, Shanghai 201804, China*

[b] *Clean Energy Automotive Engineering Center, Tongji University, Shanghai, 201804, China*

[c] *Postdoctoral Station of Mechanical Engineering, Tongji University, Shanghai, 201804, China*

[d] *Institute for Advanced Study, Tongji University, Shanghai, 200092, China*

[e] *Shanghai AI NEV Innovative Platform Co., Ltd., Shanghai, 201804, China*

Abstract

Irreversible lithium plating, as one of the unwanted side reactions, has a high risk of accelerating degradation to destroy the electrochemical performance of lithium-ion batteries (LIBs). Presently, most of the existing irreversible lithium plating detection methods are qualitative or post-mortem quantitative, and there is still a lack of an effective irreversible lithium plating in-situ quantitative detection method. Here, an in-situ quantitative irreversible lithium plating detection method within the full-lifespan of LIBs is proposed. Multi-battery parallel aging experiments are designed for the two abuse scenarios of low-temperature and high-current. By using scanning electron microscope (SEM), inductively coupled plasma-mass (ICP), and Argon-CP technology, the qualitative evolution and the quantitative detection method of irreversible lithium plating are explored. In order to make the proposed detection method non-destructive,

* Corresponding author. School of Automotive Studies, Tongji University, Shanghai, 201804, China
E-mail address: tongjidai@tongji.edu.cn (H. Dai).

Preprint not peer reviewed

This preprint research paper has not been peer reviewed. Electronic copy available at: https://ssrn.com/abstract=4292942

two in-situ factors are analyzed to establish the mapping relationship with the measured irreversible lithium plating. It makes it possible that without post-mortem, the irreversible lithium plating, for the first time, is measured quantitatively only by the in-situ factors extracted from the cycle data. Our work provides a possibility for quantitative and onboard detection of irreversible lithium plating, which is of great significance for the development of battery prognostics and health management (PHM) and echelon utilization.

Keywords: Lithium-ion battery, multi-battery parallel aging experiments, irreversible lithium plating, In-situ quantitative detection method

1 Introduction

Lithium-ion batteries (LIBs), as the main contributor to energy conservation and emission reduction policies, have been widely used in electric vehicles (EVs) and energy storage systems (EESs) in recent years [1-3]. However, a significantly longer charging time is a substantial disadvantage from the customers' perspective compared to the refueling time of gasoline vehicles. A decrease of the charging time to 15−20 min (i.e., an increase in charging current by a factor of 3 or 4) would significantly reduce the gap to refueling time and promote good development of EVs into the automotive mass market [4]. In addition, under low-temperature conditions, the cycle life and safety performance of LIBs will also be severely degraded, which has become a key bottleneck for the further development of LIBs [5-7]. In order to further improve the performance of LIBs, a large number of researches on failure mechanisms were

Preprint not peer reviewed

This preprint research paper has not been peer reviewed. Electronic copy available at: https://ssrn.com/abstract=4292942

conducted, and it was found that irreversible lithium plating is an important reason for rapid capacity degradation or even thermal runaway [8-11].

The existing safety protection monitoring indicators are usually based on battery voltage and temperature [12-14]. However, the temperature and voltage have a delayed feature when reflecting the internal state of the battery. When obvious external performance changes, preventing the battery failure by intervention or maintenance will be too late, or miss the best period. Therefore, the in-situ quantitative detection of irreversible lithium plating, as an important internal indicator, is of great significance for the improvement of battery life and safety, and can lay the foundation for the early detection of failure such as sudden drop in capacity, internal short circuit, and thermal runaway.

In recent years, a considerable effort has been made to detect irreversible lithium plating, and the methods can be divided into two categories: physical lithium plating detection method and electrochemical lithium plating detection method [15-18]. Most of physical detection methods are post-mortem methods based on the dismantled battery. Meanwhile, custom batteries such as transparent shells can be used for experiments to achieve the purpose of in-situ detection [19]. The common physical detection methods include optical methods, X-ray diffraction (XRD) methods, nuclear magnetic resonance (NMR) methods, original neutron methods, and ultrasonic detection methods. Optical detection methods such as optical microscope (OM) [20], Raman spectrum [21], scanning electron microscope (SEM) [22-24], Transmission Electron Microscope (TEM) [25, 26] and other methods [27] are mostly used for surface appearance

Preprint not peer reviewed

This preprint research paper has not been peer reviewed. Electronic copy available at: https://ssrn.com/abstract=4292942

observation of lithium plating, which is difficult to make quantitative analysis. XRD technology is widely used in the qualitative and quantitative analysis of lithium plating, and does not destroy materials [28-31]. Shui et. Al [28] applied the XRD technology to the Li-O_2 battery, which first revealed the changes of the negative electrode composition of different aging states and the different discharge depths. However, the XRD technology is often based on customized batteries, and there is a problem that the normal X-ray strength is difficult to penetrate the shell, so its application is limited. Grey et. Al [32, 33] first applied NMR technology to the Li-Li symmetrical battery to explore the internal lithium dendrites growth behavior. However, NMR technology often needs to disassemble the battery, and there is a disadvantage of irreversible damage to the battery. Ohsaki et. al [34] explored the ultrasonic non-destructive detection method of lithium plating. This research is based on the sensitivity of the ultrasonic to the gas to detect the reaction and deflation of the lithium plating and the electrolyte. However, deflation reaction is a delayed feature after lithium plating, and it cannot reflect the lithium plating state of the battery in time.

Compared with the above physical detection methods, the electrochemical detection methods have the advantages of no need to use dedicated devices, no need to customize batteries, no destructive post-mortem of batteries and have simple operation. Therefore, the electrochemical methods are also considered the ideal detection methods of lithium plating, but cannot perform quantitative detection of lithium plating. The common electrochemical detection methods include incremental capacity and differential voltage (IC-DV) method [35-40], Arrhenius method [41], internal

Preprint not peer reviewed

This preprint research paper has not been peer reviewed. Electronic copy available at: https://ssrn.com/abstract=4292942

resistance-capacity method (R-Q method) [42, 43] and distribution of relaxation times (DRT) method [44]. Smart et. al [38] identified lithium plating by discharge voltage platform, and believes that the length of voltage platform is an indicator of quantity lithium plating. Petzl et. al [39] analyze the discharge curve to obtain the IC curve, and diagnose lithium plating by observing whether there is a minimal value. The Arrhenius method believes that the battery capacity degradation is completely derived from the lithium plating and the growth of solid electrolyte interphase (SEI) film. If the capacity aging does not comply with the Arrhenius Standard, it is considered that the capacity degradation is caused by the growth of the SEI and the lithium plating, which proves the occurrence of lithium plating. Zhang et. al [43] used the R-Q method to diagnose whether the lithium plating has occurred. Because the electrical conductivity of lithium metal precipitated on the negative surface is better than the SEI film, when the degree of capacity degradation is the same, the battery with lithium plating has less internal resistance. Therefore, the trends in the R-Q curve can know whether the lithium plating has occurred.

Although there have been researches of the lithium plating detection discussed above, there are still some obstacles that need to be further overcome. (1) Most of the detection methods are ex-situ, and the battery needs to be disassembled. Even if the lithium plating can be analyzed quantitatively, the discontinuing of the battery information is not allowed to be applied to the online analysis of LIBs. (2) Most of the in-situ methods can only analyze lithium plating qualitatively, but not quantitatively. (3) Reversible and irreversible lithium plating cannot be distinguished. In fact, irreversible

Preprint not peer reviewed

This preprint research paper has not been peer reviewed. Electronic copy available at: https://ssrn.com/abstract=4292942

lithium plating is the key reason causing rapid capacity degradation, which will damage the battery health and safety performance [45]. Therefore, there is currently badly in need of an in-situ method for LIBs to detect and quantify irreversible lithium plating within the full-lifespan.

In this paper, a battery in-situ quantitative detection method of irreversible lithium plating was proposed. Aimed at the low-temperature and high-current application scenarios, the multi-battery parallel aging experiment and post-mortem experiment of irreversible lithium plating detection are designed. By using the scanning electron microscope (SEM), inductively coupled plasma-mass (ICP) and Argon-CP technology, the qualitative evolution of lithium plating and the quantitative detection method of irreversible lithium are explored. Meanwhile, in order to make the irreversible lithium plating detection method non-destructive, two optimal in-situ characterization factors were selected and analyzed, then the mapping relationship between the in-situ characterization factors and the measured irreversible lithium plating is established, so that the amount of irreversible lithium plating can be directly measured by the voltage and impedance information. This work fills the blank of the in-situ quantitative detection of irreversible lithium plating for LIBs, which makes important contributions to battery prognostics and health management (PHM) and safety early warning.

2 Experiments

Low-temperature and high-current charging conditions can easily induce battery lithium plating, resulting in the accumulation of irreversible lithium deposition. In this

Preprint not peer reviewed

This preprint research paper has not been peer reviewed. Electronic copy available at: https://ssrn.com/abstract=4292942

paper, for extreme abuse conditions of low-temperature and high-current, two groups of the multi-battery parallel aging experiment were designed, as schematically illustrated in **Fig. 1**. Each experimental group uses 8 batteries, which are calibrated and disassembled at different aging stages, and the capacity calibration and impedance calibration experiments are performed on all cells to observe whether the consistency of the health state for all cells is stable. Through the calibration experiments, we use IC-DV, EIS, and DRT approaches to extract the battery multi-dimensional features to obtain the potential in-situ characteristic factor of irreversible lithium plating. Immediately afterwards, we fully discharged, disassembled, and characterized the battery in turn, which guarantees that the negative electrode of the dismantling cell does not include reversible lithium deposition. Through ICP, SEM and argon-ion cutting and polishing (Argon-CP) approaches, the battery irreversible lithium plating is detected and quantified.

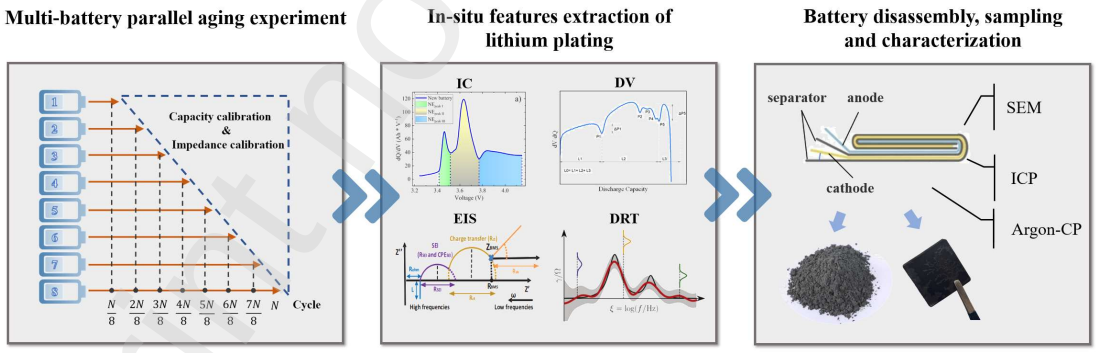

Fig. 1. Battery aging and characterization experimental procedures.

Through the above procedures, under the premise of ensuring a strong consistency of parallel aging cells, we can obtain the continuous evolution process of the external feature factors and internal irreversible lithium plating within the whole aging process, which solves the discontinuity of in-situ and ex-situ information caused by battery post-

Preprint not peer reviewed

This preprint research paper has not been peer reviewed. Electronic copy available at: https://ssrn.com/abstract=4292942

mortem. The cell information and detailed procedures in the experiment will be introduced in the following content.

2.1 Lithium-ion cells and cycling environment

The experimental cells in this paper are customized soft package batteries. The positive electrode material is $LiNi_{0.8}Co_{0.1}Mn_{0.1}O_2$ (NCM811) and the negative electrode material is graphite. The commercial electrolyte of 1 mol $LiPF_6$ was used, and also contains two other solvents: ethylene carbonate (EC) and diethyl carbonate (DEC), and their weight content is 12.36%, 43.82%, and 43.82%. The rated capacity of the customized battery is 1Ah, the charging cut-off voltage is 4.2V, and the discharge cut-off voltage is 3V.

The positive and negative tabs of the experimental cells are connected to the load and sampling end of the battery charging and discharge test system (Maccor), and the thermostat is used to maintain the constant temperature. The experimental cells are performed by the aging test with constant current and constant voltage (CC-CV), as shown in **Fig. 2**A, and the detailed steps of low-temperature aging and high-current aging conditions are shown in **Table 1** and **Table 2**.

Table 1

Low-temperature aging experimental steps

No.	Steps	Current (A)	End condition	Temperature (℃)
1	Rest		4h	-5
2	CC charge	0.5	Cut-off voltage: 4.2V	-5

Preprint not peer reviewed

This preprint research paper has not been peer reviewed. Electronic copy available at: https://ssrn.com/abstract=4292942

3	CV charge		Cut-off current: 0.02A	-5
4	Rest		4h	-5
5	CC discharge	0.5	Cut-off voltage: 3V	-5
6	CV discharge		Cut-off current: 0.02A	-5
7			Repeat the above steps	

Table 2

High-current aging experimental steps

No.	Steps	Current (A)	End condition	Temperature (℃)
1	Rest		2h	25
2	CC charge	4.5	Cut-off voltage: 4.2V	25
3	CV charge		Cut-off current: 0.02A	25
4	Rest		2h	25
5	CC discharge	2	Cut-off voltage: 3V	25
6	CV discharge		Cut-off current: 0.02A	25
7			Repeat the above steps	

2.2 Capacity calibration and impedance calibration experiment

All battery calibration experiments mentioned above will be performed using rated current and at room temperature. The purpose is to extract the feature factors of aging and detect the consistency of the remaining cells. The low-temperature group is calibrated every 30-90 cycles, while the high-current group of the normal temperature is calibrated every 20-50 cycles. The specific cyclic interval is adjusted according to

Preprint not peer reviewed

This preprint research paper has not been peer reviewed. Electronic copy available at: https://ssrn.com/abstract=4292942

the battery state of health (SoH). In order to enable the IC-DV method to extract effective feature factors, the calibration current is 0.1A. The impedance calibration used the equipment of TOYO Corporation China and tested the battery at 50% state of charge (SoC). The test stand is shown in **Fig. 2**B.

2.3 Cell post-mortem and characterization experiment

The post-mortem experiment is the prerequisite for various ex-situ characterization experiments of LIBs. The post-mortem of the battery needs to be performed in the conjoined glove box filled with argon to prevent the sample from oxidizing or pollution. As shown in **Fig. 2**C, the conjoined glove box (MBRAUN-MB-200B-MOD) provides an environment to isolate the air, which is full of inert gases. The battery that completed the calibration experiment will be sent into the glove box, and be disassembled and sampled.

After the disassembly procedure, three characterization methods were used to explore the quantification of irreversible lithium deposition, namely SEM, ICP and Argon-CP, respectively. The surfaces of the positive electrode, negative electrode and separator were observed through SEM (JEOL JSM-7610FPLUS), thereby confirming the occurrence of lithium plating, as shown in **Fig. 2**D. In addition, the sample needs to be cut and polished to obtain its horizontal cross-section, and the obtained horizontal cross-section also needs to be observed by SEM, and the CP device (IB-19520CCP) is shown in **Fig. 2**E. In order to detect the content of lithium and phosphorus in the sample, the ICP (VARIAN 720-ES) is used.

Preprint not peer reviewed

This preprint research paper has not been peer reviewed. Electronic copy available at: https://ssrn.com/abstract=4292942

In particular, in order to ensure that the sample is always in the vacuum environment during the transfer from glove boxes to SEM, the vacuum transfer box needs to be used, as shown in **Fig. 2**F. Similarly, for the ion beam cutting, the cross-section polishing instrument requires the sample to expose 100 microns of the sample holder. To achieve this goal, it is necessary to use a sample installation tool adapter, prominent tools, and a sample holder, as shown in **Fig. 2**G.

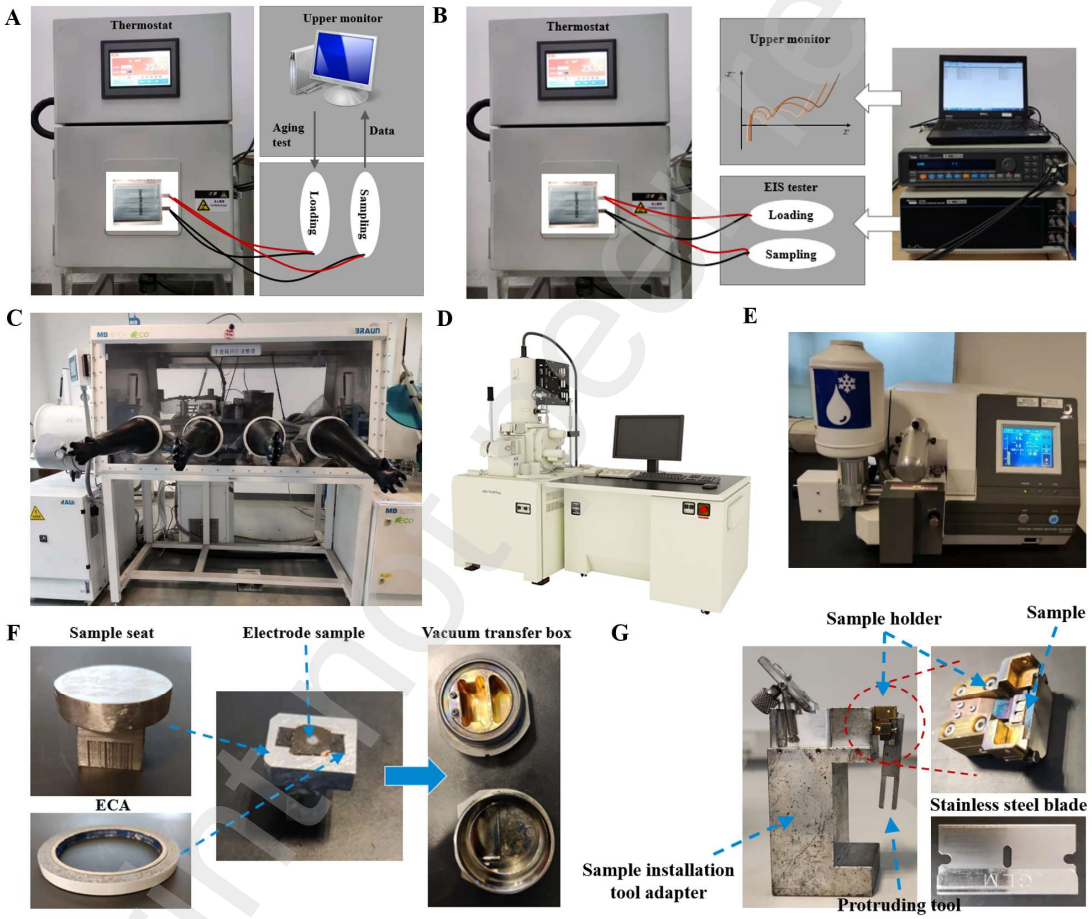

Fig. 2. Lithium-ion battery aging, calibration and characterization experimental equipment.

Preprint not peer reviewed

This preprint research paper has not been peer reviewed. Electronic copy available at: https://ssrn.com/abstract=4292942

3 Results and discussion

3.1 Irreversible lithium plating quantitative detection method

With the rapid aging of LIBs under extreme operating conditions, the irreversible lithium deposition is gradually accumulating, and the quantitative detection of irreversible lithium plating has become a core problem. Focusing on this problem, by using SEM, ICP and Argon-CP technology, the qualitative evolution of lithium plating on the anode and the quantitative detection method of irreversible lithium are explored. Taking the low-temperature group as an example, the macroscopic and microscopic morphological changes of the electrode surfaces under different aging levels are analyzed, as shown in **Fig. 3**.

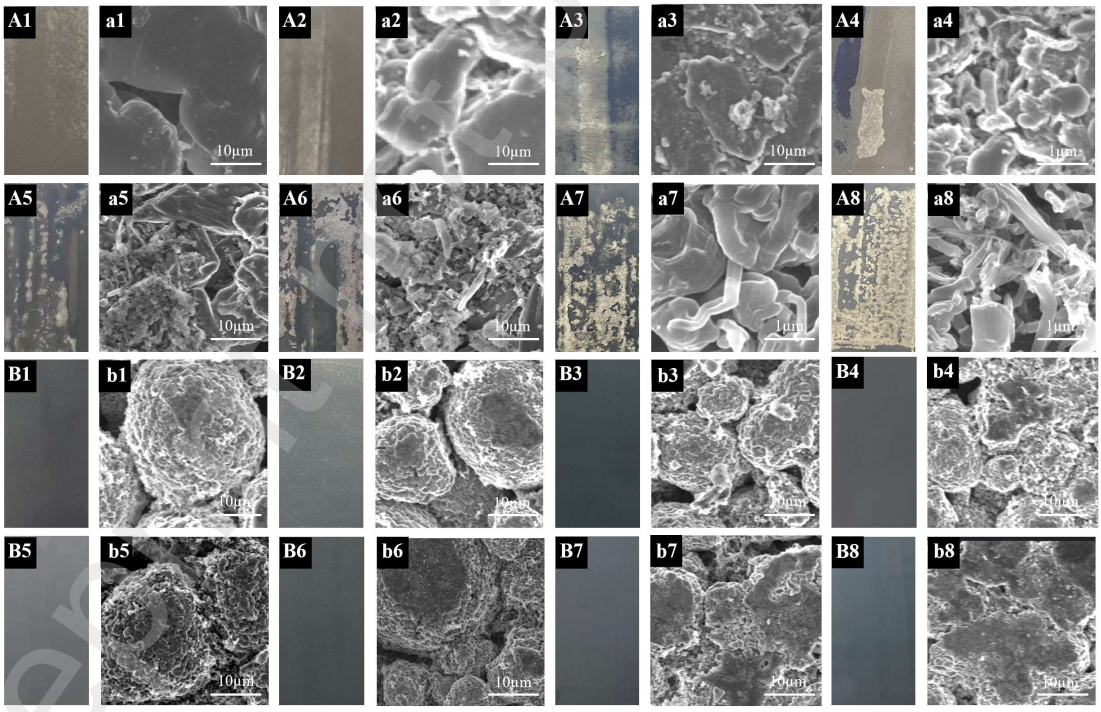

Fig. 3. Surface appearances and SEM images of cathode and anode of low-temperature group. (A, a) The anode surface appearances and SEM images of the 8 cells in low-temperature group, the

Pre-print peer reviewed

This preprint research paper has not been peer reviewed. Electronic copy available at: https://ssrn.com/abstract=4292942

numbers of 1-8 correspond to the order of post-mortem respectively; (B, b) The cathode surface appearances and SEM images of the 8 cells in low-temperature group, the numbers of 1-8 correspond to the order of post-mortem respectively.

For the anode, as shown in **Fig. 3**A(1-8) it can be seen from a macroscopic point of view that white depositions appear on the surface of the graphite. This white deposition is formed by the slow oxidation of the precipitated lithium element, that is, lithium plating. And as the battery aging, the coverage area of the white deposition increases, indicating that the lithium plating becomes more serious. From the microscopic point of view, through SEM, a large number of lithium dendrites can be seen in the white deposition area. For the cathode, as shown in **Fig. 3**B(1-8), there is no obvious change with aging on the macroscopic scale, the surface is still smooth, and the positive electrode material is tightly bonded to the current collector. From the microscopic level, there is a very thin film on the surface of the positive electrode particles, which is also called cathode electrolyte interphase (CEI) film.

In addition, in order to explore the internal state, the samples of the battery anode and cathode were cut by Argon-CP technique, and the cross-sectional morphologies of two electrodes were obtained. Combined with the SEM technique under high magnification, the cross-section and surface film thickness of the electrodes were explored. Here, the representative cross-sectional images of the low-temperature group were selected for analysis, as shown in **Fig. 4**. From **Fig. 4**A and **4**B, the diameter of the cathode particles is about 5-20μm, and some of the particles are broken, which may be caused by aging or the battery manufacture. During the whole experiment, the

Preprint not peer reviewed

This preprint research paper has not been peer reviewed. Electronic copy available at: https://ssrn.com/abstract=4292942

thickness of the CEI film was difficult to measure. In **Fig. 4**C, after 480 cycles, the film thickness was only about 30-60nm.

Compared with the cathode, the SEM cross-sectional morphology of the battery anode provides more valuable information. In **Fig. 4**D the graphite material is separated from the current collector, which may also be one of the reasons for the serious aging of the battery. In **Fig. 4**E, a very thick lithium deposition layer is formed on the surface of the negative electrode, with a thickness of about 20μm. In addition, in **Fig. 4**F, we observed that there are also lithium depositions wrapped by oxide films between the inner graphite particles. These products not only consume the recyclable lithium, but also cause the decrease of the electrode porosity. More interestingly, extensive observations of the cross-section of the graphite anode show that the existence of the SEI film on the graphite surface is a common phenomenon, and as the battery ages, the SEI film will thicken. Therefore, we performed statistical measurements on the film thickness of the low-temperature and high-current groups, respectively, and obtained the thickness change of the SEI film with aging. **Fig. 4**(G-I) show the SEI film thickness observed after the post-mortem of the low-temperature battery at 60 cycles, 270 cycles and 540 cycles, respectively, and the thickness increased from 99 nm to about 250 nm. **Fig. 4**(J-L) show the SEI film thickness after the post-mortem of the high-current battery at 50 cycles, 100 cycles and 200 cycles, respectively, and the thickness increased from 80 nm to about 220 nm.

Preprint not peer reviewed

This preprint research paper has not been peer reviewed. Electronic copy available at: https://ssrn.com/abstract=4292942

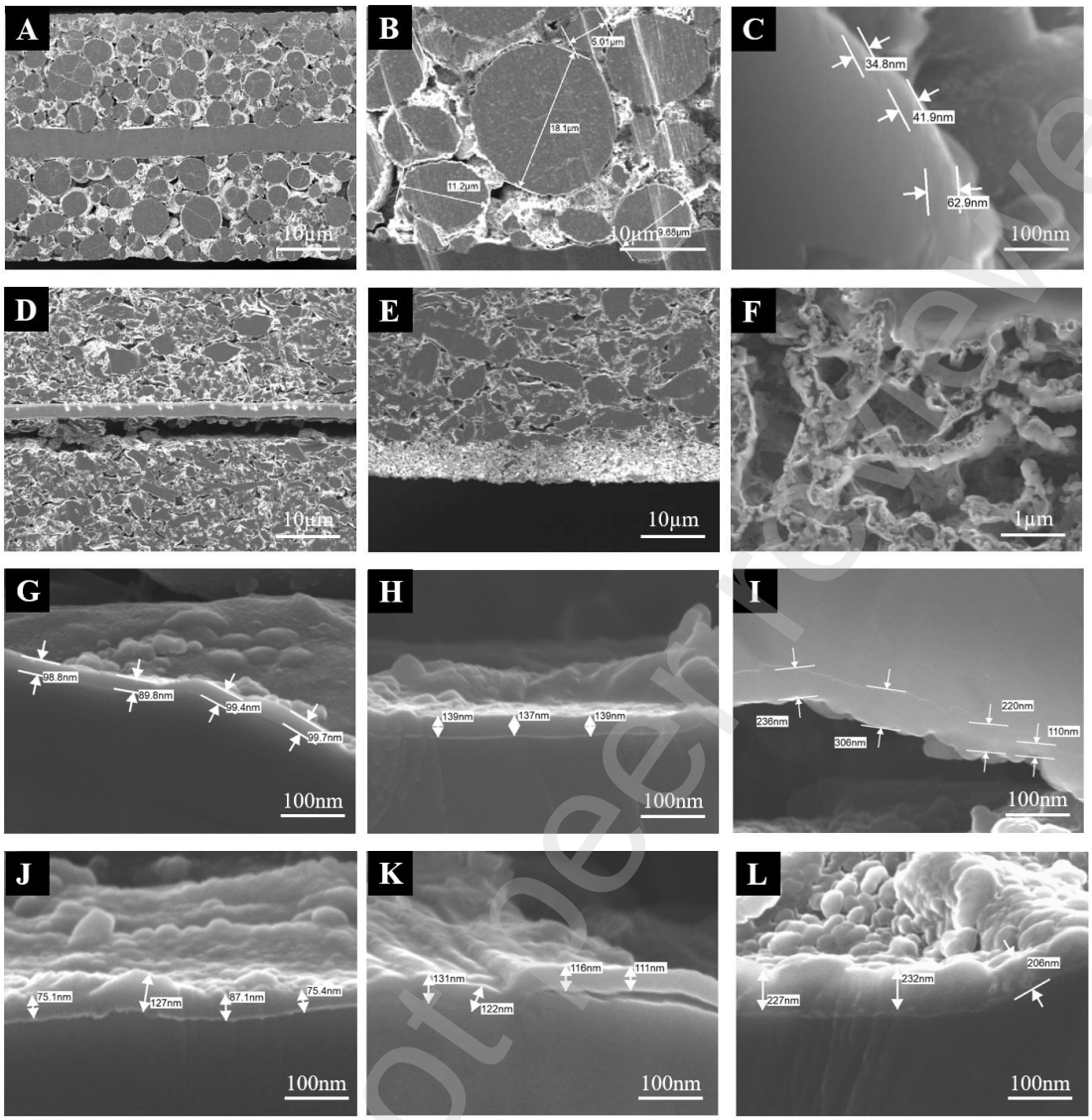

Fig. 4. The anode and cathode cross-sectional images of the low-temperature group by SEM-Argon-CP.

It can be seen that the SEI film thickness increases gradually with the aging of the battery. Therefore, in order to further explore the quantitative relationship between SEI film thickness and battery aging, several cells were selected in each of the two experimental groups, and four sampling areas are selected on the negative electrode of each cell, the SEI film thickness of the four points is measured, and the average thickness of the four sampling areas is taken as the SEI film thickness of the battery,

Preprint not peer reviewed

This preprint research paper has not been peer reviewed. Electronic copy available at: https://ssrn.com/abstract=4292942

and the measurement results are shown in **Fig. 5**(A-C). Among them, **Fig. 5**A and **Fig. 5**B are the box distribution and gaussian distribution of the measured SEI film thickness for the low-temperature and the high-current groups under a fixed number of cycles. **Fig. 5**C shows the change of SEI film thickness, which can be seen that the change rate of SEI film thickness of the two groups are slowing down with battery aging.

In order to quantitatively detect the irreversible lithium plating of LIBs, the quantitative measurement of the irreversible lithium loss (ILL) contained in the anode is required. In particular, before post-mortem, the anode is discharged using a CV strategy with 0.02A cut-off current, and the anode at this time is approximately in a fully discharged state. Therefore, the ILL in the anode detected by the ICP mainly includes three categories, namely, ILL in the SEI film, ILL in the lithium plating, and ILL in the lithium salts, as shown in **Fig. 5**D. **Fig. 5**E shows the total ILL contained in the anode detected by ICP, and the ILL of the low-temperature group and the high-current group at each aging level are very close. It is worth noting that during the ICP test of the anode, the contents of two elements, Li and P, were measured. The reason is that the lithium salts in the electrolyte will still be attached to the fully discharged anode, and these lithium elements will also be detected by the ICP. Since the electrolyte we used only contains one lithium-containing electrolyte, namely $LiPF_6$, and the ratio of Li to P is 1:1, so the amount of P can be used to exclude the errors caused by the Li in the lithium salt to the measurement result, and the lithium content evolution contained in the lithium salts is shown in **Fig. 5**F Therefore, we have excluded the lithium content in lithium salts through the measurement of the P element, and as long as the ILL in the

Preprint not peer reviewed

This preprint research paper has not been peer reviewed. Electronic copy available at: https://ssrn.com/abstract=4292942

SEI film is excluded, the rest is completely ILL in the lithium plating, that is, irreversible lithium plating.

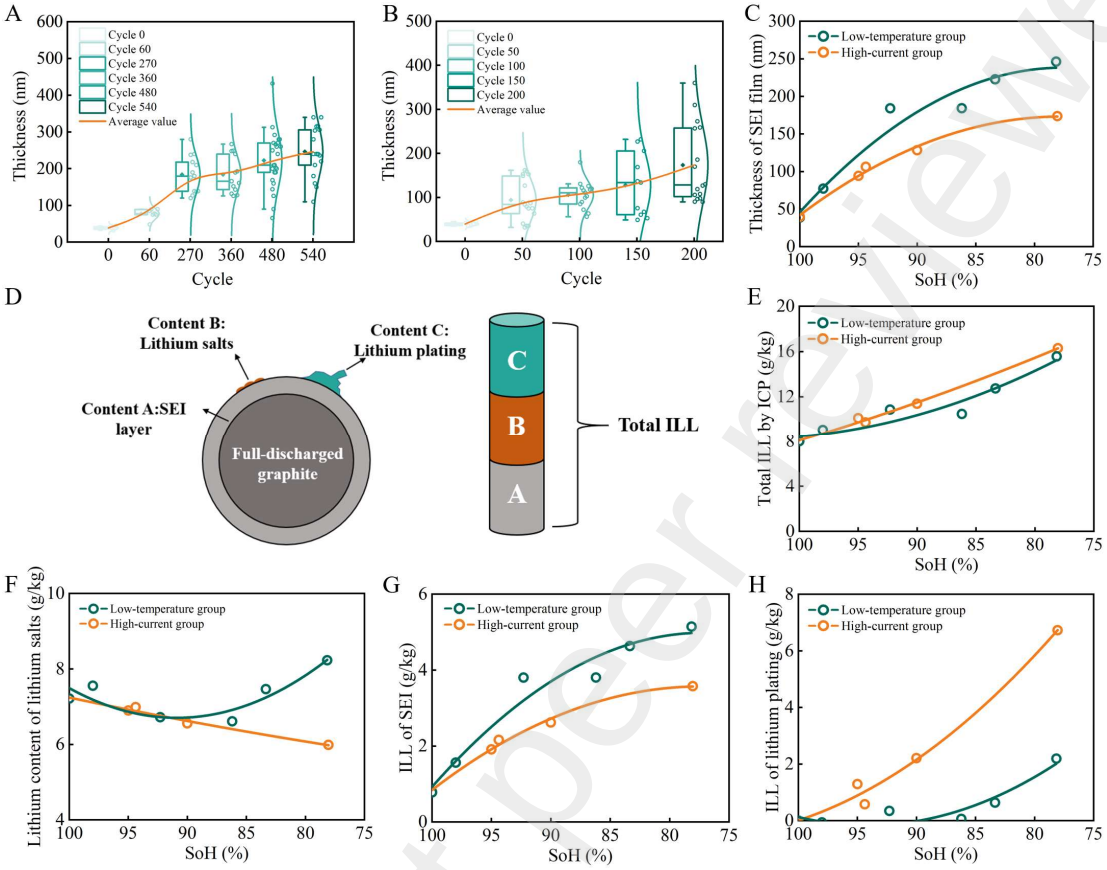

Fig. 5. Quantitative measurement of irreversible lithium loss of the two experimental groups. (A) Statistical box image and normal distribution curve of SEI film thickness of the low-temperature group; (B) Statistical box image and normal distribution curve of SEI film thickness of the high-current group; (C) The Fitted curve of average thickness evolution with aging; (D) ILL composition of fully discharged; (E) Total ILL of anode measured by ICP; (F) Lithium content in lithium salts; (G) ILL of SEI film; (H) ILL of lithium plating.

Here, based on the research of previous outstanding scholars [46, 47], the graphite particles are hypothesized to be spheres, and the SEI film grows on the surface of the spheres. By measuring the average thickness of the SEI film, we assumed that the SEI film produced a film of uniform thickness on the surface of the sphere. In addition, in

Preprint not peer reviewed

This preprint research paper has not been peer reviewed. Electronic copy available at: https://ssrn.com/abstract=4292942

general, there is no lithium plating in the battery at cycle 0, and the lithium content measured by ICP at this time is all derived from the SEI film and lithium salts. Therefore, the ratio of the amount of lithium element to the volume of the SEI film at this time is the content of lithium element in the SEI film per unit volume, and the ILL contained in the SEI film and the irreversible lithium plating are calculated by Equations (1) and (2), and their quantitative evolution is shown in **Fig. 5**G and **Fig. 5**H.

$$Li_{SEI} = (Li_{ICP,0\ cycle} - Li_{Salt}) \times \frac{\frac{4}{3}\pi((r+\Delta d_{i\ cycle})^3 - r^3)}{\frac{4}{3}\pi((r+\Delta d_{0\ cycle})^3 - r^3)} \quad (1)$$

$$Li_{Plating} = Li_{ICP} - Li_{SEI} - Li_{Salt} \quad (2)$$

where Li_{SEI} is the ILL in the SEI film, $Li_{ICP,0\ cycle}$ is the ILL of the anode at full discharge measured by ICP at 0 cycle, Li_{Salt} is the lithium content in the lithium salt measured by ICP, r is the average radius of the graphite particles, which is 10.82μm obtained from the cross-section measurement obtained by SEM-Argon-CP, i is the number of aging cycles for the disassembled battery, and $Li_{Plating}$ is the ILL of lithium plating.

Based on the above methods, the ILL contained in the lithium plating and SEI film has been quantitatively detected, and its evolution at different aging levels has also been explored. Comparing **Fig. 5**G and **Fig. 5**H, in both two conditions, the growth rate of ILL caused by SEI is decreasing with aging, while the growth rate of ILL caused by lithium plating is increasing. It is worth noting that the ILL caused by lithium plating detected in the method is irreversible lithium plating.

Preprint not peer reviewed

This preprint research paper has not been peer reviewed. Electronic copy available at: https://ssrn.com/abstract=4292942

3.2 The extraction and analysis of in-situ characterization factor

In order to make the irreversible lithium plating detection method non-destructive, five in-situ characterization factors were selected and analyzed to establish the mapping relationship between the in-situ characterization factors and the measured irreversible lithium plating. For online applications of LIBs, the battery voltage and impedance are definitely the most informative. Therefore, in this paper, the IC-DV, EIS, and DRT methods were used for voltage data and impedance data to extract in-situ characterization factors, respectively. Taking the low-temperature group as an example, the characterization factors at different aging levels and their correlation with the irreversible lithium plating measured in the previous section are shown in **Fig. 6**.

The IC-DV method is widely used in the research field of battery aging, which is obtained through the differential of charging or discharge curve. In the IC-DV curve, the height changes and position offset of peak valley have a close connection with the aging mechanism. Therefore, many scholars have quantified their curve characteristics with the help of three mechanism-related degradation modes (DMs) of loss of lithium inventory (LLI), loss of active material (LAM) and conductivity loss (CL) [48, 49]. As shown in **Fig. 6**A and **Fig. 6**B, the maximum voltage U_{max} in the IC curve quantifies the CL, the maximum capacity Q_{max} in the DV curve is used to quantify LLI, and the peak value $\frac{\Delta Q}{\Delta U}$, which is related to LAM in the IC curve, is used to quantify LAM. Eventually, the quantitative formulas of three DMs based on IC-DV methods are as follows.

$$CL = \frac{U_{max,fresh} - U_{max,aging}}{U_{max,fresh}} \times 100\% \quad (3)$$

Preprint, not peer reviewed

This preprint research paper has not been peer reviewed. Electronic copy available at: https://ssrn.com/abstract=4292942

$$LLI = \frac{Q_{max,fres} - Q_{max,aging}}{Q_{max,fresh}} \times 100\% \quad (4)$$

$$LAM = \frac{\frac{\Delta Q}{\Delta U_{fresh}} - \frac{\Delta Q}{\Delta U_{aging}}}{\frac{\Delta Q}{\Delta U_{fresh}}} \times 100\% \quad (5)$$

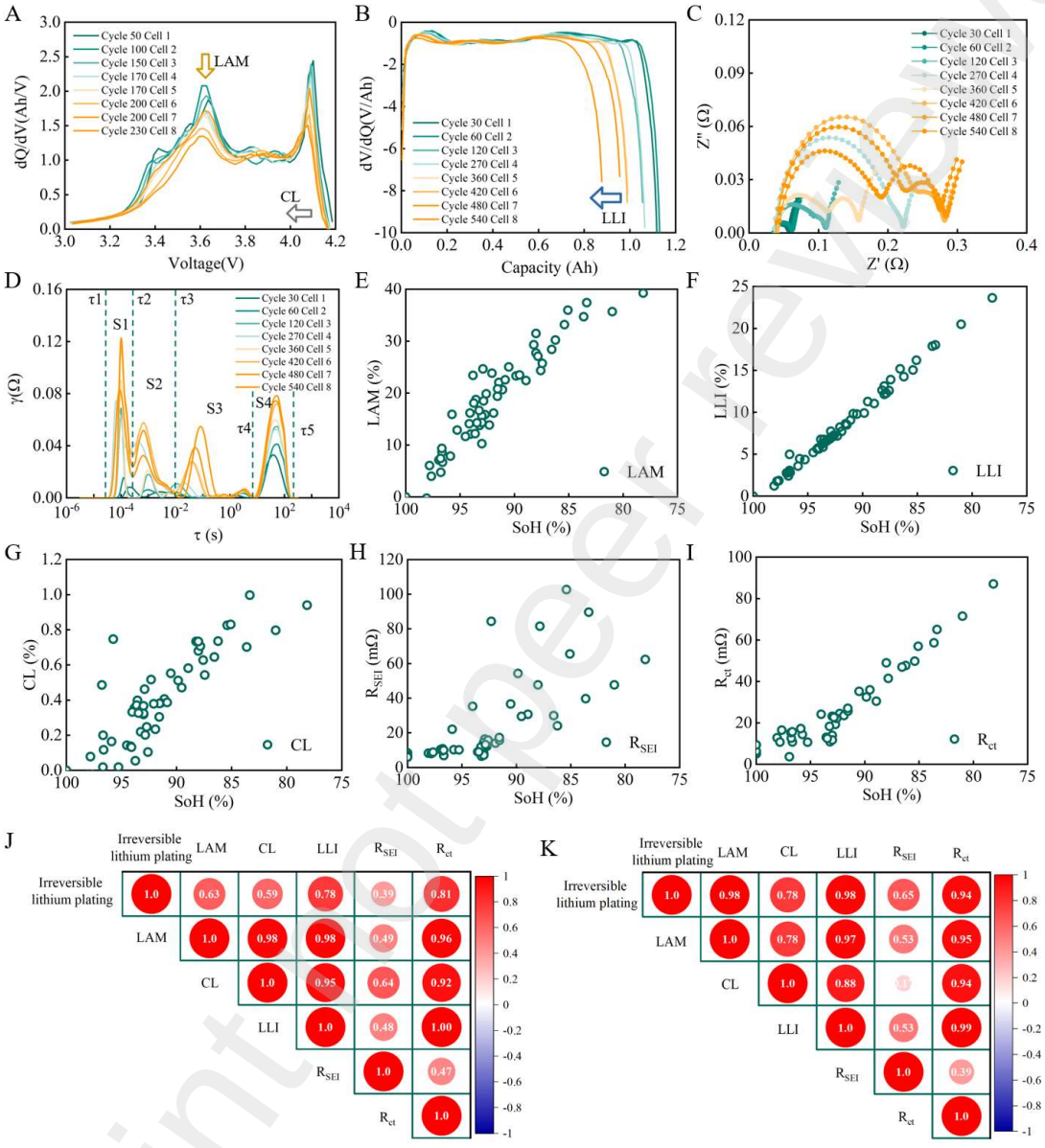

Fig. 6. In-situ characterization factor extraction and correlation analysis. (A) IC curves of low-temperature group; (B) DV curves of low-temperature group; (C) EIS curves of low-temperature group; (D) DRT curves of low-temperature group; (E) Quantitative results of LAM; (F) Quantitative results of LLI; (G) Quantitative results of CL; (H) Quantitative results of R_{SEI}; (I) Quantitative results of R_{ct}; (J) Correlation heatmap analysis of irreversible lithium plating and in-situ

Preprint not peer reviewed

This preprint research paper has not been peer reviewed. Electronic copy available at: https://ssrn.com/abstract=4292942

characterization factors of low-temperature group; (K) Correlation heatmap analysis of irreversible lithium plating and in-situ characterization factors of high-rate group.

Unlike the IC-DV method, the EIS method focuses more on the power characteristics of the battery, and the impedance of the battery at different frequencies will be in-depth analyzed. According to the experimental scheme, the frequency range of 0.01Hz to 10kHz is selected, which not only guarantees that the EIS has an intersection point with the horizontal axis and can characterize the Ohmic resistance, and at the same time, the ultra-high frequency part is not too long. In addition, the changing trend of EIS under different SoCs is basically the same, and 50% SoC data is selected here to introduce in detail, and the EIS information of eight low-temperature batteries is shown in **Fig. 6**C.

However, EIS always needs to be analyzed in combination with the equivalent circuit model (ECM) [50, 51] to characterize the internal electrochemical process through parameter recognition. At the same time, the same EIS data with different ECMs can be fitted to different results, which makes the analysis results of EIS often filled with vagueness and uncertainty [52, 53]. In order to solve the above problems, DRT has been proposed and widely used in the related issues of analyzing battery aging [54]. DRT can determine the number of time constants and their frequency range, which greatly reduces the uncertainty in EIS analysis. Different electrochemical processes have different relaxation time distributions, so DRT analysis can be used to distinguish different electrochemical processes. DRT can be used to separate and quantify the polarization process into four resistances [55], namely ohm resistance R_{ohm}, contact

Preprint not peer reviewed

This preprint research paper has not been peer reviewed. Electronic copy available at: https://ssrn.com/abstract=4292942

resistance R_c, interface resistance R_i and diffusion resistance R_d. Furthermore, the interface resistance R_i is related to the charge transmission and charge transfer reactions, and it is divided into SEI film resistance R_{SEI} and transfer resistance R_{ct}. As shown **Fig. 6**D, the DRT curve consists of S1, S2, S3 and S4, which corresponds to R_c, R_{SEI}, R_{ct} and R_d, and the time constant range is $\tau_1 - \tau_2$, $\tau_2 - \tau_3$, $\tau_3 - \tau_4$ and $\tau_4 - \tau_5$ respectively [54]. It should be noted that the R_{ohm} cannot be characterized by the DRT curve, and its resistance value can be directly calculated through the DRT tool [56].

Based on the above methods, from the voltage and impedance information, five in-situ characterization factors that are positively correlated with irreversible lithium plating were selected, which is LAM, LLI, CL, R_{SEI} and R_{ct}. And their evolution with the aging of the battery is shown in **Fig. 6**(E-I). As can be seen from the figure, the five characterization factors all show an increasing trend with the aging of the battery, which is positively correlated with the change trend of measured irreversible lithium plating. Furthermore, **Fig. 6**J and **Fig. 6**K are correlation heat maps of the low-temperature group and the high-current group between the characteristic factors and the measured irreversible lithium plating, respectively. For low-temperature group batteries, the two characteristic factors of LLI and R_{ct} have the strongest correlation with irreversible lithium plating. For the high-current group, the correlation coefficient between LAM, LLI, R_{ct} and irreversible lithium plating was higher than 0.94. For LLI, it is an indicator to describe the loss of active lithium ions, and the loss of active lithium ions is closely related to irreversible lithium plating, especially when the battery enters the

Preprint not peer reviewed

This preprint research paper has not been peer reviewed. Electronic copy available at: https://ssrn.com/abstract=4292942

nonlinear aging. Therefore, there is a strong correlation between LLI and irreversible lithium plating. R_{ct} is related to the charge transfer process in the battery, which is also closely related to the irreversible lithium plating. The greater the resistance of R_{ct}, the more difficult the insertion reaction of lithium ions in the negative electrode will be, which will easily lead to lithium plating. For LAM, it is related to the structural transformation of active material and the decomposition of electrolytes. The loss of active material will also lead to the reduction of the recyclable active lithium ions. However, LAM only has a strong correlation with irreversible lithium plating at high current condition, while this correlation is weak for low-temperature aging batteries. Therefore, in order to make the extracted characterization factors adapt to both low-temperature and high-current conditions, herein, the LLI extracted by the voltage data and the R_{ct} extracted by the impedance data are selected as the optimal in-situ quantitative characterization factors of the irreversible lithium plating.

3.3 Lithium-ion battery full-lifespan irreversible lithium plating in-situ quantitative detection method and online service framework

Based on the multiple-battery parallel aging experiment, the quantitative measurement of irreversible lithium plating and its corresponding optimal in-situ characterization factors of low-temperature group and high-current group under different aging levels are obtained, respectively. Combined with the above optimal in-situ quantitative characterization factors of LLI and R_{ct}, an in-situ quantitative irreversible lithium plating detection method in the entire lifespan of LIBs is proposed.

Preprint not peer reviewed

This preprint research paper has not been peer reviewed. Electronic copy available at: https://ssrn.com/abstract=4292942

Fig. 7A and **Fig. 7**B are the mapping relationships between the characteristic factors of LLI and R_{ct} and irreversible lithium plating under low-temperature condition, respectively. **Fig. 7**C is its quantitative equation, and through this equation, the true irreversible lithium plating of battery with similar working conditions can be known without post-mortem analysis, only through the simple processing of voltage data or impedance data. For the battery of the high-current group, as shown in **Fig. 7**(D-F), the mapping relationship and quantitative equation between the in-situ characteristic factors and the irreversible lithium plating are also established. In addition, for the battery of low-temperature groups, due to the small charging current, the irreversible lithium plating is almost non-cumulative in the early stage. For the battery of the high-current group, the lithium plating situation occurs earlier and is more serious.

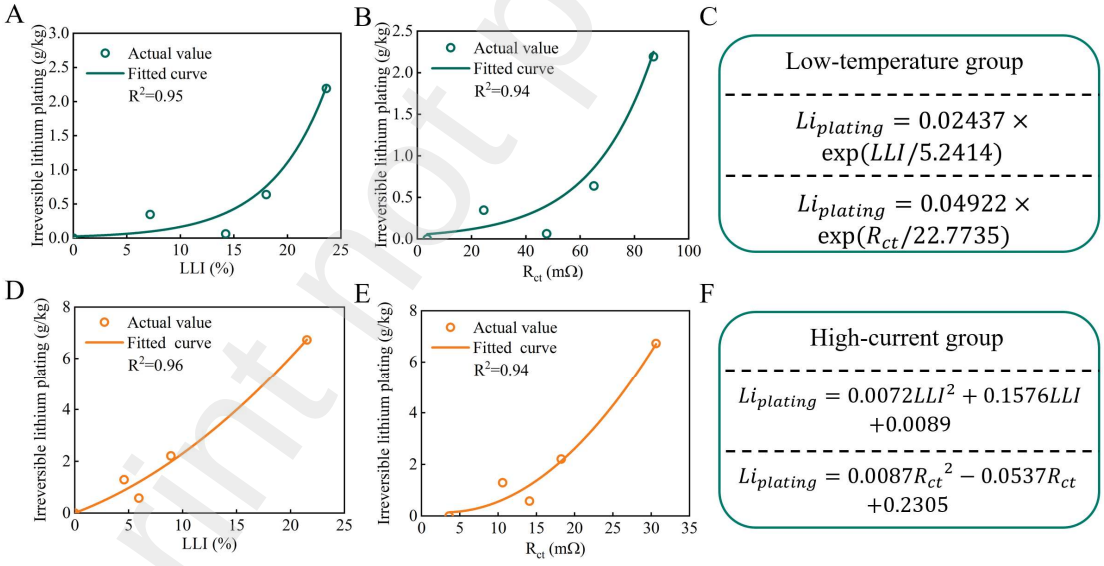

Fig. 7. Relationship and quantitative equation between irreversible lithium plating and in-situ factors of two experimental groups (A) Relationship curve of irreversible lithium plating characterized by LLI of low-temperature group; (B) Relationship curve of irreversible lithium plating characterized by R_{ct} of low-temperature group; (C) In-situ quantitative detection equation

Preprint not peer reviewed

This preprint research paper has not been peer reviewed. Electronic copy available at: https://ssrn.com/abstract=4292942

for irreversible lithium plating of low-temperature group; (D) Relationship curve of irreversible lithium plating characterized by LLI of high-current group; (E) Relationship curve of irreversible lithium plating characterized by R_{ct} of high-current group; (F) In-situ quantitative detection equation for irreversible lithium plating of high-current group.

From the above analysis, it can be seen that two typical specific working conditions (-5℃, 0.5A and 25℃, 4.5A) are taken from the low-temperature and high-current conditions for in-situ quantitative detection of irreversible lithium plating. And from the results, the two influencing factors of temperature and current have different effects on the lithium plating side reaction of the battery. When the battery is only in one of the extreme working conditions of low-temperature or high-current, the irreversible lithium plating can be quantified in-situ directly through the conclusions obtained herein. Meanwhile, since the method obtains the ILL per unit of anode active material, the method is applicable to various types of batteries under the same anode material. However, when faced with the coupling of non-standard temperature and non-standard current, the quantitative equation of the in-situ quantitative detection method of irreversible lithium plating should also be coupled, which requires a lot of experiments to verify. Surely, the experimental design and process proposed in this work are suitable for quantitative exploration of irreversible lithium plating under other working conditions. In non-standard temperature and non-standard current condition, researchers can use our proposed experimental process to obtain the in-situ quantitative detection method of irreversible lithium plating by making corresponding working condition experiments.

Preprint not peer reviewed

This preprint research paper has not been peer reviewed. Electronic copy available at: https://ssrn.com/abstract=4292942

Furthermore, based on the in-situ quantitative irreversible lithium plating detection method proposed, an online LIB full-lifespan irreversible lithium plating quantitative detection service framework is built, as shown in **Fig. 8**. To our knowledge, this work is the first attempt to quantify the irreversible lithium plating of LIBs online. The accumulation of irreversible lithium plating will not only cause rapid capacity degradation, but also may cause nonlinear aging and safety failure problems of the battery. Therefore, the development of this online irreversible lithium plating quantitative detection helps to enrich the dimensions of online battery information in addition to voltage, temperature, current, impedance, etc., which makes important contributions to the in-depth battery modeling, PHM, and accurate estimation of various nonlinear states.

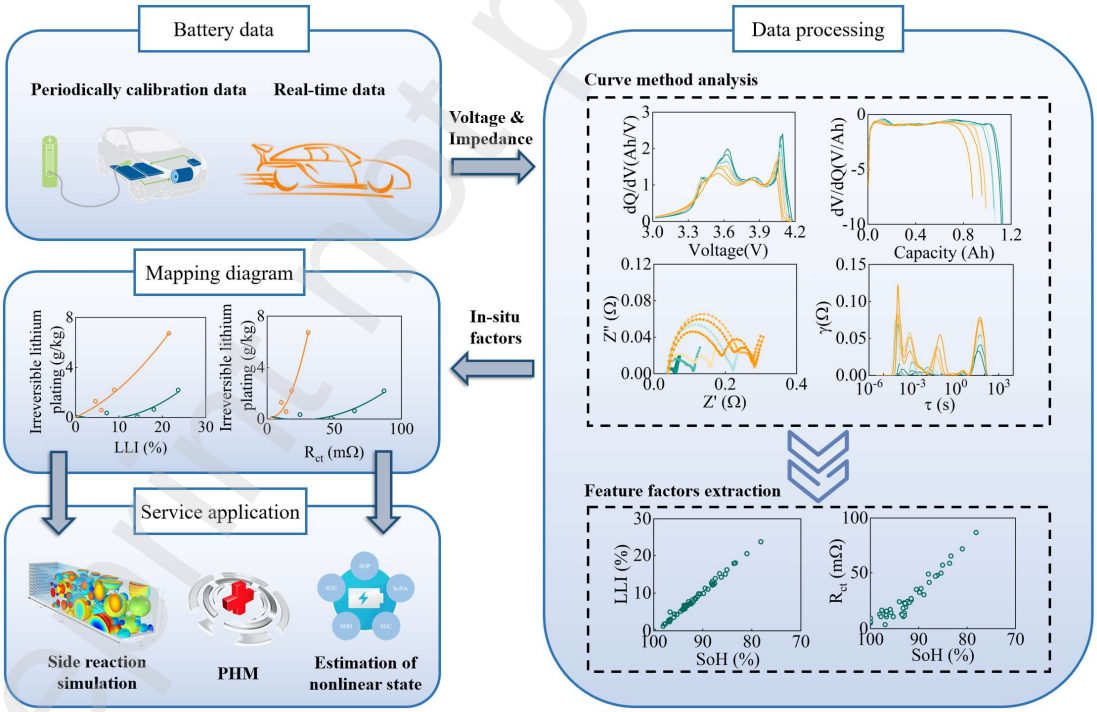

Fig. 8. The online LIB full-lifespan irreversible lithium plating quantitative detection service framework.

This preprint research paper has not been peer reviewed. Electronic copy available at: https://ssrn.com/abstract=4292942

4 Conclusion

Irreversible lithium plating is an important reason for the rapid aging of LIBs, and it may also lead to serious safety hazards. Only by knowing the degree of irreversible lithium plating inside the battery can we accurately evaluate the actual aging and safety status of LIBs. However, at present, the amount of irreversible lithium plating can only be qualitatively analyzed by some in-situ methods, that is, knowing whether it occurs or quantitative analysis by post-mortem of the battery.

In this paper, an in-situ quantitative detection method for irreversible lithium plating is proposed. By designing multi-battery parallel aging experiments, the evolution process of irreversible lithium plating inside the battery was explored, which solves the discontinuity of battery information caused by the post-mortem process. In addition, through SEM, Argon-CP and ICP, the qualitative detection method for the amount of irreversible lithium plating was proposed. In order to make the irreversible lithium plating detection method non-destructive, combined with IC-DV, EIS and DRT methods, two optimal in-situ characterization factors were selected and analyzed to establish the mapping relationship between the in-situ characterization factors and the measured irreversible lithium plating. Ultimately, without post-mortem, it is the first time that the irreversible lithium plating inside the battery is measured quantitatively only by the in-situ characteristic factor extracted from the cycle data. Furthermore, we apply our in-situ quantitative irreversible lithium plating detection method to build an online LIB full-lifespan irreversible lithium plating quantitative detection service framework, which provides an important basis for online real-time full-lifespan aging

Preprint not peer reviewed

This preprint research paper has not been peer reviewed. Electronic copy available at: https://ssrn.com/abstract=4292942

state evaluation and fault diagnosis of LIBs in EVs, EESs and echelon utilization. Moreover, importantly, the method is expected to be extended to other battery material systems other than LIBs, which will make important contributions to the development of the battery applications.

Declaration of Competing Interest

The authors declare that they have no known competing financial interests or personal relationships that could have appeared to influence the work reported in this paper.

Data availability

Data will be made available on request.

Acknowledgment

This work is financially supported by the National Natural Science Foundation of China (NSFC, Grant No. U20A20310) and Program of Shanghai Academic/ Technology Research Leader (22XD1423800), and also sponsored by the National Natural Science Foundation of China (NSFC, Grant No. 52107230, No. 52176199)

References

[1] M.-K. Tran, M. Fowler, A Review of Lithium-Ion Battery Fault Diagnostic Algorithms: Current Progress and Future Challenges, Algorithms, 13 (2020).

Preprint not peer reviewed

This preprint research paper has not been peer reviewed. Electronic copy available at: https://ssrn.com/abstract=4292942

[2] W. Xie, X. Liu, R. He, Y. Li, X. Gao, X. Li, Z. Peng, S. Feng, X. Feng, S. Yang, Challenges and opportunities toward fast-charging of lithium-ion batteries, J. Energy Storage, 32 (2020).

[3] W. Sun, Diagnose lithium battery, Nat. Nanotechnol., 13 (2018) 436-436.

[4] K.G. Gallagher, S.E. Trask, C. Bauer, T. Woehrle, S.F. Lux, M. Tschech, P. Lamp, B.J. Polzin, S. Ha, B. Long, Q. Wu, W. Lu, D.W. Dees, A.N. Jansen, Optimizing Areal Capacities through Understanding the Limitations of Lithium-Ion Electrodes, J. Electrochem. Soc., 163 (2015) A138-A149.

[5] B. Liu, Y. Jia, C. Yuan, L. Wang, X. Gao, S. Yin, J. Xu, Safety issues and mechanisms of lithium-ion battery cell upon mechanical abusive loading: A review, Energy Storage Mater., 24 (2020) 85-112.

[6] R. Schmuch, R. Wagner, G. Hörpel, T. Placke, M. Winter, Performance and cost of materials for lithium-based rechargeable automotive batteries, Nat. Energy, 3 (2018) 267-278.

[7] H. You, J. Zhu, X. Wang, B. Jiang, H. Sun, X. Liu, X. Wei, G. Han, S. Ding, H. Yu, W. Li, D.U. Sauer, H. Dai, Nonlinear health evaluation for lithium-ion battery within full-lifespan, J. Energy Chem., 72 (2022) 333-341.

[8] U.R. Koleti, A. Rajan, C. Tan, S. Moharana, T.Q. Dinh, J. Marco, A Study on the Influence of Lithium Plating on Battery Degradation, Energies, 13 (2020).

[9] T. Ma, D. Xu, M. Wei, H. Wu, X. He, Z. Zhang, D. Ma, S. Liu, B. Fan, C. Lin, L. Liu, F. Wang, Study on lithium plating caused by inconsistent electrode decay rate during aging of traction batteries, Solid State Ionics, 345 (2020).

[10] M.W. Verbrugge, D.R. Baker, The influence of surface inhomogeneity on the overcharge and lithium plating of graphite electrodes, J. Phys Energy, 2 (2019).

[11] G. Zhang, X. Wei, X. Tang, J. Zhu, S. Chen, H. Dai, Internal short circuit mechanisms, experimental approaches and detection methods of lithium-ion batteries for electric vehicles: A review, Renew, Sust.

Preprint not peer reviewed

This preprint research paper has not been peer reviewed. Electronic copy available at: https://ssrn.com/abstract=4292942

Energ. Rev., 141 (2021).

[12] W. Mei, L. Zhang, J. Sun, Q. Wang, Experimental and numerical methods to investigate the overcharge caused lithium plating for lithium ion battery, Energy Storage Mater., 32 (2020) 91-104.

[13] I.D. Campbell, M. Marzook, M. Marinescu, G.J. Offer, How Observable Is Lithium Plating? Differential Voltage Analysis to Identify and Quantify Lithium Plating Following Fast Charging of Cold Lithium-Ion Batteries, J. Electrochem. Soc., 166 (2019) A725-A739.

[14] B. Jiang, H. Dai, X. Wei, Incremental capacity analysis based adaptive capacity estimation for lithium-ion battery considering charging condition, Appl. Energy, 269 (2020).

[15] X.-L. Gao, X.-H. Liu, W.-L. Xie, L.-S. Zhang, S.-C. Yang, Multiscale observation of Li plating for lithium-ion batteries, Rare Metals, 40 (2021) 3038-3048.

[16] U. Janakiraman, T.R. Garrick, M.E. Fortier, Review—Lithium Plating Detection Methods in Li-Ion Batteries, J. Electrochem. Soc., 167 (2020).

[17] Y. Tian, C. Lin, H. Li, J. Du, R. Xiong, Detecting undesired lithium plating on anodes for lithium-ion batteries – A review on the in-situ methods, Appl. Energy, 300 (2021).

[18] D. Liu, Z. Shadike, R. Lin, K. Qian, H. Li, K. Li, S. Wang, Q. Yu, M. Liu, S. Ganapathy, X. Qin, Q.H. Yang, M. Wagemaker, F. Kang, X.Q. Yang, B. Li, Review of Recent Development of In Situ/Operando Characterization Techniques for Lithium Battery Research, Adv. Mater., 31 (2019).

[19] Z. Deng, X. Lin, Z. Huang, J. Meng, Y. Zhong, G. Ma, Y. Zhou, Y. Shen, H. Ding, Y. Huang, Recent Progress on Advanced Imaging Techniques for Lithium-Ion Batteries, Adv. Energy Mater., 11 (2020).

[20] F. Ringbeck, C. Rahe, G. Fuchs, D.U. Sauer, Identification of Lithium Plating in Lithium-Ion Batteries by Electrical and Optical Methods, J. Electrochem. Soc., 167 (2020).

[21] T. Rauhala, K. Jalkanen, T. Romann, E. Lust, N. Omar, T. Kallio, Low-temperature aging

Preprint not peer reviewed

This preprint research paper has not been peer reviewed. Electronic copy available at: https://ssrn.com/abstract=4292942

mechanisms of commercial graphite/LiFePO4 cells cycled with a simulated electric vehicle load profile—A post-mortem study, J. Energy Storage, 20 (2018) 344-356.

[22] G. Zhang, X. Wei, G. Han, H. Dai, J. Zhu, X. Wang, X. Tang, J. Ye, Lithium plating on the anode for lithium-ion batteries during long-term low temperature cycling, J. Power Sources, 484 (2021).

[23] Y. Wang, C. Zhang, J. Hu, P. Zhang, L. Zhang, L. Lao, Investigation on calendar experiment and failure mechanism of lithium-ion battery electrolyte leakage, J. Energy Storage, 54 (2022).

[24] Y. Chen, L. Torres-Castro, K.-H. Chen, D. Penley, J. Lamb, M. Karulkar, N.P. Dasgupta, Operando detection of Li plating during fast charging of Li-ion batteries using incremental capacity analysis, J. Power Sources, 539 (2022).

[25] L. Geng, C. Zhao, J. Yan, C. Fu, X. Zhang, J. Yao, H. Sun, Y. Su, Q. Liu, L. Zhang, Y. Tang, F. Ding, J. Huang, In situ imaging the dynamics of sodium metal deposition and stripping, J. Mater. Chem. A, 10 (2022) 14875-14883.

[26] Y. Li, X. Li, J. Chen, C. Cai, W. Tu, J. Zhao, Y. Tang, L. Zhang, G. Zhou, J. Huang, In Situ TEM Studies of the Oxidation of Li Dendrites at High Temperatures, Adv. Funct. Mater., 32 (2022).

[27] K.N. Wood, E. Kazyak, A.F. Chadwick, K.H. Chen, J.G. Zhang, K. Thornton, N.P. Dasgupta, Dendrites and Pits: Untangling the Complex Behavior of Lithium Metal Anodes through Operando Video Microscopy, ACS Cent. Sci., 2 (2016) 790-801.

[28] S. Jiang Lan, O. John S., K. Peter, D. Howard A., Z. Dan, A. Jonathan D., L. Di Jia, Reversibility of anodic lithium in rechargeable lithium–oxygen batteries, Nat. Commun., 4 (2013).

[29] K.P.C. Yao, J.S. Okasinski, K. Kalaga, I.A. Shkrob, D.P. Abraham, Quantifying lithium concentration gradients in the graphite electrode of Li-ion cells using operando energy dispersive X-ray diffraction, Energ. Environ. Sci., 12 (2019) 656-665.

Preprint not peer reviewed

This preprint research paper has not been peer reviewed. Electronic copy available at: https://ssrn.com/abstract=4292942

[30] P.P. Paul, C. Cao, V. Thampy, H.-G. Steinrück, T.R. Tanim, A.R. Dunlop, S.E. Trask, A.N. Jansen, E.J. Dufek, J. Nelson Weker, M.F. Toney, Using In Situ High-Energy X-ray Diffraction to Quantify Electrode Behavior of Li-Ion Batteries from Extreme Fast Charging, ACS Appl. Energ. Mater., 4 (2021) 11590-11598.

[31] K. Sato, A. Tamai, K. Ohara, H. Kiuchi, E. Matsubara, Non-destructive observation of plated lithium distribution in a large-scale automobile Li-ion battery using synchrotron X-ray diffraction, J. Power Sources, 535 (2022).

[32] R. Bhattacharyya, B. Key, H. Chen, A.S. Best, A.F. Hollenkamp, C.P. Grey, In situ NMR observation of the formation of metallic lithium microstructures in lithium batteries, Nat. Mater., 9 (2010) 504-510.

[33] H.J. Chang, A.J. Ilott, N.M. Trease, M. Mohammadi, A. Jerschow, C.P. Grey, Correlating Microstructural Lithium Metal Growth with Electrolyte Salt Depletion in Lithium Batteries Using (7)Li MRI, J. Am. Chem. Soc., 137 (2015) 15209-15216.

[34] T. Ohsaki, T. Kishi, T. Kuboki, N. Takami, N. Shimura, Y. Sato, M. Sekino, A. Satoh, Overcharge reaction of lithium-ion batteries, J. Power Sources, 146 (2005) 97-100.

[35] W. Mei, L. Jiang, C. Liang, J. Sun, Q. Wang, Understanding of Li-plating on graphite electrode: detection, quantification and mechanism revelation, Energy Storage Mater., 41 (2021) 209-221.

[36] A. Adam, E. Knobbe, J. Wandt, A. Kwade, Application of the differential charging voltage analysis to determine the onset of lithium-plating during fast charging of lithium-ion cells, J. Power Sources, 495 (2021).

[37] M. Koseoglou, E. Tsioumas, D. Ferentinou, I. Panagiotidis, N. Jabbour, D. Papagiannis, C. Mademlis, Lithium plating detection using differential charging current analysis in lithium-ion batteries, J. Energy Storage, 54 (2022).

Preprint not peer reviewed

This preprint research paper has not been peer reviewed. Electronic copy available at: https://ssrn.com/abstract=4292942

[38] M.C. Smart, B.V. Ratnakumar, Effects of Electrolyte Composition on Lithium Plating in Lithium-Ion Cells, J. Electrochem. Soc., 158 (2011) A379-A389.

[39] M. Petzl, M. Kasper, M.A. Danzer, Lithium plating in a commercial lithium-ion battery – A low-temperature aging study, J. Power Sources, 275 (2015) 799-807.

[40] B. Jiang, H. Dai, X. Wei, A Cell-to-Pack State Estimation Extension Method Based on a Multilayer Difference Model for Series-Connected Battery Packs, IEEE T. Transp. Electr., 8 (2022) 2037-2049.

[41] T. Waldmann, M. Wilka, M. Kasper, M. Fleischhammer, M. Wohlfahrt-Mehrens, Temperature dependent ageing mechanisms in Lithium-ion batteries – A Post-Mortem study, J. Power Sources, 262 (2014) 129-135.

[42] L. Xu, Y. Yang, Y. Xiao, W.-L. Cai, Y.-X. Yao, X.-R. Chen, C. Yan, H. Yuan, J.-Q. Huang, In-situ determination of onset lithium plating for safe Li-ion batteries, J. Energy Chem., 67 (2022) 255-262.

[43] Z. Yakun, L. Xinyu, S. Laisuo, L. Zhe, L. Boryann, Z. Jianbo, Lithium Plating Detection and Quantification in Li-Ion Cells from Degradation Behaviors, ECS Trans., 75 (2017) 37-50.

[44] Y. Mengchao, J. Fachao, Z. Guangjin, G. Dongxu, R. Dongsheng, L. Languang, O. Minggao, Detection of lithium plating based on the distribution of relaxation times, 2021 IEEE 4th International Electrical and Energy Conference (CIEEC), (2021).

[45] X.-G. Yang, Y. Leng, G. Zhang, S. Ge, C.-Y. Wang, Modeling of lithium plating induced aging of lithium-ion batteries: Transition from linear to nonlinear aging, J. Power Sources, 360 (2017) 28-40.

[46] S. Das, P.M. Attia, W.C. Chueh, M.Z. Bazant, Electrochemical Kinetics of SEI Growth on Carbon Black: Part II. Modeling, J. Electrochem. Soc., 166 (2019) E107-E118.

[47] A. Wang, S. Kadam, H. Li, S. Shi, Y. Qi, Review on modeling of the anode solid electrolyte interphase (SEI) for lithium-ion batteries, npj Comput. Mater., 4 (2018).

Preprint not peer reviewed

This preprint research paper has not been peer reviewed. Electronic copy available at: https://ssrn.com/abstract=4292942

[48] M. Dubarry, C. Truchot, B.Y. Liaw, Synthesize battery degradation modes via a diagnostic and prognostic model, J. Power Sources, 219 (2012) 204-216.

[49] C. Pastor-Fernández, K. Uddin, G.H. Chouchelamane, W.D. Widanage, J. Marco, A Comparison between Electrochemical Impedance Spectroscopy and Incremental Capacity-Differential Voltage as Li-ion Diagnostic Techniques to Identify and Quantify the Effects of Degradation Modes within Battery Management Systems, J. Power Sources, 360 (2017) 301-318.

[50] D. Andre, M. Meiler, K. Steiner, H. Walz, T. Soczka-Guth, D.U. Sauer, Characterization of high-power lithium-ion batteries by electrochemical impedance spectroscopy. II: Modelling, J. Power Sources, 196 (2011) 5349-5356.

[51] B. Jiang, J. Zhu, X. Wang, X. Wei, W. Shang, H. Dai, A comparative study of different features extracted from electrochemical impedance spectroscopy in state of health estimation for lithium-ion batteries, Appl. Energy, 322 (2022).

[52] F. Ciucci, Modeling electrochemical impedance spectroscopy, Curr. Opin. Electrochem., 13 (2019) 132-139.

[53] J. Huang, Z. Li, B.Y. Liaw, J. Zhang, Graphical analysis of electrochemical impedance spectroscopy data in Bode and Nyquist representations, J. Power Sources, 309 (2016) 82-98.

[54] X. Zhou, J. Huang, Z. Pan, M. Ouyang, Impedance characterization of lithium-ion batteries aging under high-temperature cycling: Importance of electrolyte-phase diffusion, J. Power Sources, 426 (2019) 216-222.

[55] I.-T. Ellen, W. André, Evaluation of electrochemical impedance spectra by the distribution of relaxation times, J. Ceram. Soc. Jpn., 125 (2017) 1-4.

[56] J. Liu, F. Ciucci, The Gaussian process distribution of relaxation times: A machine learning tool for

Preprint not peer reviewed

This preprint research paper has not been peer reviewed. Electronic copy available at: https://ssrn.com/abstract=4292942

the analysis and prediction of electrochemical impedance spectroscopy data, Electrochim. Acta, 331 (2020).

Preprint not peer reviewed

This preprint research paper has not been peer reviewed. Electronic copy available at: https://ssrn.com/abstract=4292942